Multi-level structural modeling of an offshore wind turbine

Francesco Petrini[1], Konstantinos Gkoumas*[1], Wensong Zhou[2] and Hui Li[2]

[1]School of Engineering, Sapienza Università di Roma, Via Eudossiana 18, Rome, Italy
[2]School of Civil Engineering, Harbin Institute of Technology, 202 Haihe Road, Nan'gang District, Harbin 150090, China

Abstract. Offshore wind turbines are complex structural and mechanical systems located in a highly demanding environment. This paper proposes a multi-level system approach for studying the structural behavior of the support structure of an offshore wind turbine. In accordance with this approach, a proper numerical modeling requires the adoption of a suitable technique in order to organize the qualitative and quantitative assessment in various sub-problems, which can be solved by means of sub-models at different levels of detail, both for the structural behavior and for the simulation of loads. Consequently, in a first place, the effects on the structural response induced by the uncertainty of the parameters used to describe the environmental actions and the finite element model of the structure are inquired. After that, a meso-level FEM model of the blade is adopted in order to obtain the detailed load stress on the blade/hub connection.

Keywords: probabilistic analysis; performance-based design; uncertainty propagation; rotating blades

1. Introduction

Offshore wind farms are the next step in the evolution of wind energy (Hau 2006, Breton and Moe 2009) and are becoming increasingly popular renewable energy option around the globe. Offshore wind turbines (OWT) have many advantages in comparison with onshore wind turbines. In fact, their operation takes advantage of the presence of regular and strong wind and their environmental impact is limited since they are located far away from the coast. An OWT is composed by mechanical and structural elements, and cannot be considered an ordinary civil engineering system. It has different configurations according to the operating conditions (in service or idle), is subject to time-varying strong actions, like wind, waves and sea currents, and can be brought into the nonlinear range.

An additional aspect is that, even if OWT's are not designed to resist every unforeseeable critical event or arbitrarily high accidental action, they should be able to maintain integrity and a certain level of functionality under accidental circumstances. Actually, the resistance of these structures to exceptional actions is addressed in codes and standards but it is often not supported with a comprehensive description of feasible methods to improve and verify this requirement (Giuliani and Bontempi 2010).

According the multi-level modeling philosophy adopted in this study (Petrini *et al.* 2010), with

---

*Corresponding author, Associate Researcher, E-mail: konstantinos.gkoumas@uniroma1.it

respect to macro-level models, meso-level models take into account the effects obtained by a more detailed description of the shape of the structural components. A high level of details in the modeling of the actions supports the highest level of detail the structural parts modeling. This multi-level approach is nowadays common practice in the Structural Health Monitoring of complex structural systems (Arangio and Bontemp 2010), and can be further developed using soft computing methods such as Bayesian neural networks (see for example Arangio and Beck 2010).

Considering what said, the design of complex structures such as an OWT is based frequently on the results of deterministic structural analyses carried out on finite element models of the structural system. However, the assessment of the structural response is affected by a significant uncertainty due to the random variability of both the environmental actions and the geometric and mechanical properties of the structure. Neglecting pertinent sources of uncertainty may lead to an incorrect evaluation of the stochastic properties of the structural response, and thus, to an improper risk assessment for a given structure subjected to a specific hazard.

For these systems, for which there are significant dependencies among elements or subsystems, it is important to have a solid knowledge of both how the system works as a whole, within the global concept of Dependability, a concept that describes the aspects assumed as relevant about the quality performance and its influencing factors (Arangio et al. 2010).

Therefore, the assessment of the Aeolian and hydrodynamic risk of an OWT has to be carried out in probabilistic terms, considering the different sources of uncertainty characterizing both the actions and the structural properties and the effects of the interaction between the wind field, the waves, the sea current and the structure (Bontempi 2006).

A procedure for the design of OWTs has been developed in the framework of Performance-Based Wind Engineering (Petrini 2009, Petrini and Ciampoli 2011) and a classification of the various sources of uncertainty is discussed: Fig. 1 (Ciampoli et al. 2011) provides an overview.
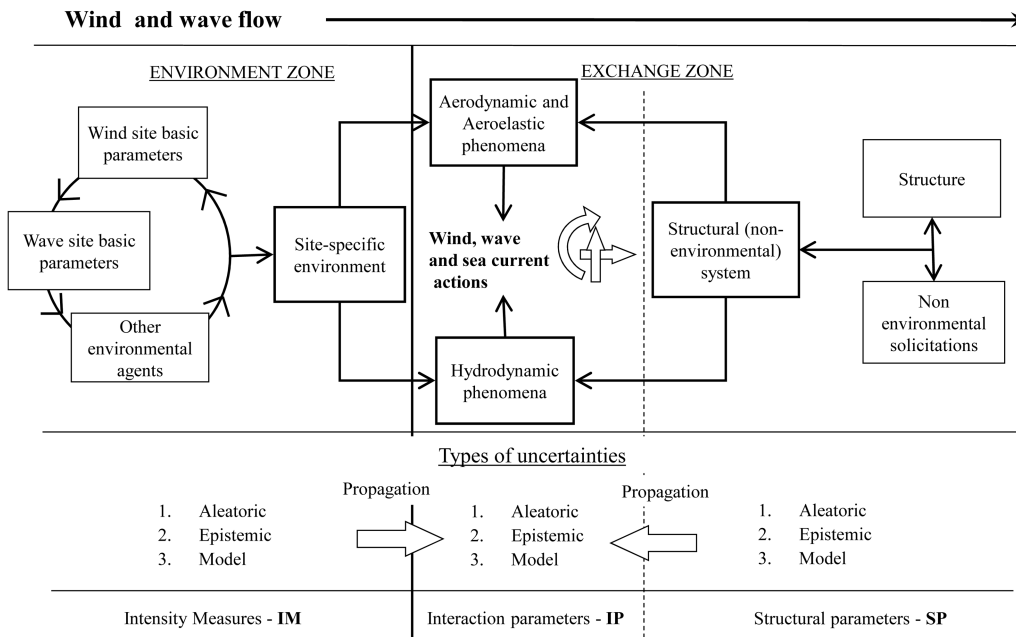

Fig. 1 Sources of uncertainty in the Performance-Based Design of Offshore wind turbines

This classification suggests a number of assumptions regarding the uncertainty propagation, where the formal representation of the propagation is expressed in terms of conditional probabilities. The result of the procedure is a set of probabilistic relations between the stochastic parameters characterizing the input and the structural response.

For a structure subject to wind and hydrodynamic actions, two zones can be distinguished:

• the environment zone, comprising the region characterized by uniform environmental parameters, where it is possible to neglect the perturbation of the flow fields due to the presence of the structure itself;

• the exchange zone, comprising the region where the effects of the wind-fluid-structure interaction cannot be neglected.

In general three sources of uncertainty have to be considered: (i) the intrinsic variability of the dynamic characteristics of the structure and the basic parameters of the wind, wave and sea current fields, arising e.g. from the unpredictable nature of magnitude and direction of the wind velocity and turbulence intensity (the *inherent* or *aleatory* uncertainty); (ii) the errors associated to the experimental measures and the incompleteness of data and information (the *epistemic* uncertainty); (iii) the modeling of wind, waves and sea current actions and their effects on the structural response (the *model* uncertainty).

The interaction parameters in the exchange zone (e.g., the aerodynamic polar lines, the aeroelastic derivatives and the Strouhal number) are strongly dependent on the basic parameters that characterize the environmental actions; in their probabilistic characterization, the uncertainties of the basic parameters defining the environment must be properly taken into account. Other parameters do not depend on the basic parameters, and their aleatory uncertainty can be considered negligible in comparison with that of the basic parameters: examples are some mechanical properties of the structure.

In what follows, the (uncertain) basic parameters that characterize the environment are grouped in the so-called Intensity Measure (**IM**) vector; the uncertain parameters of interest in the exchange zone are grouped in the two vectors of derived interaction **IP** and independent structural **SP** parameters. If the limit state is quantified in terms of an Engineering Demand Parameter EDP, the procedure simply requires the evaluation of the complementary cumulative distribution function (CCDF) of EDP

$$G(EDP) = \int_{-\infty}^{\infty} G(EDP|\mathbf{IM}, \mathbf{IP}, \mathbf{SP}) \cdot f(\mathbf{IP}|\mathbf{IM}, \mathbf{SP}) \cdot f(\mathbf{IM}) \cdot f(\mathbf{SP}) \cdot d\mathbf{IM} \cdot d\mathbf{IP} \cdot d\mathbf{SP} \qquad (1)$$

There are several methods for computing the integral (1). In the numerical example illustrated in this study, a crude Monte Carlo simulation is used.

A proper probability characterization of the parameters is assumed, and the relevance and the propagation of the uncertainty to the response are investigated. The results presented in this paper are useful for a preliminary design phase, in which upper and lower bounds of the stochastic structural response have to be estimated in order to select the best design configuration among alternative ones.

2. Aerodynamic and hydrodynamic actions

The hydrodynamic action models are illustrated in Petrini *et al.* (2010a) and Petrini *et al.* (2010b). Usually, if an environmental action is described on the basis of observations obtained with reference to a short period of time, it can be described by a deterministic mean component that is constant or slowly varying with time, and by a random fluctuating component. If aerodynamic and hydrodynamic actions are considered, the former component is evaluated by considering the mean wind velocity and the sea current, while the fluctuating component is generated by the turbulent wind velocity and the irrotational waves (with the exception of the breaking waves). The mean component varies in a stochastic manner if long periods are considered (e.g., one year). For this reason, in what follows the mean component will be considered deterministic only if the structural response is evaluated with reference to a short period of time.

The elements governing the design of OWTs are described in Fig. 2 (Petrini *et al.* 2010a). The relevant geometric parameters are: the mean water depth from still water level (h), the hub height above the still water level (H) and the blade length or rotor radius (R).

The variation of the mean velocity V_m with the height z over a horizontal surface of homogeneous roughness can be described by an exponential law

$$V_m(z) = V_{hub} \cdot \left(\frac{z}{z_{hub}} \right)^k \tag{2}$$

where V_{hub} is the 10-minute mean wind velocity at the height of the rotor z_{hub}, and k is a site-dependent parameter that can be taken equal to 0.14 for extreme wind conditions (DNV 2010).

The 10-minute wind velocity V_{hub} is defined as a function of the return period T_R. This is the $(1-1/T_R)$ percentile of the distribution of the annual maximum 10-minute mean wind velocity, i.e., the 10-minute mean wind velocity whose probability of exceedance in 1 year is $1/T_R$. It is given by
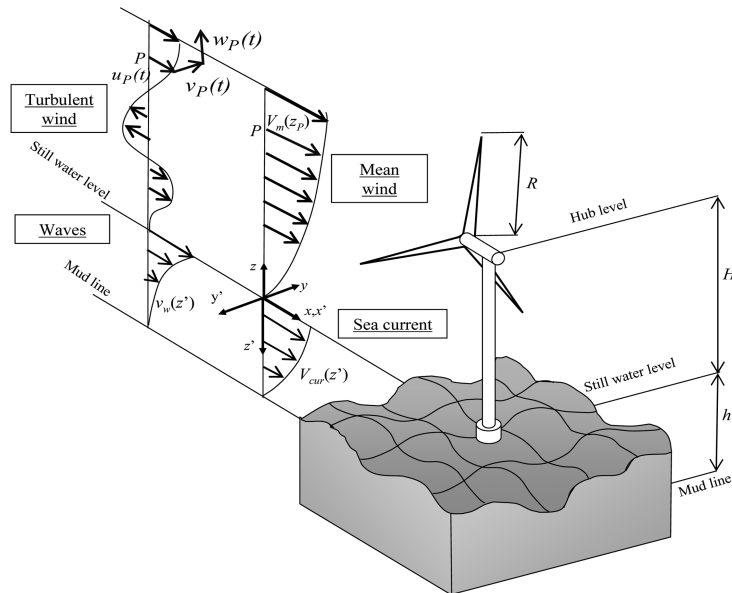

Fig. 2 Schematic representation of the elements governing the design of offshore wind turbines

$$V_{hub} = F_{V_{hub},max,1year}^{-1}\left(1-\frac{1}{T_R}\right) \tag{3}$$

where TR > 1 year and $_{FVhub,max,1year}(\bullet)$ is the cumulative distribution function of the annual maximum value of the 10-minute mean wind velocity.

The turbulent components of the wind velocity can be modeled as zero-mean Gaussian ergodic independent processes by making use of well-known formulations (Carassale and Solari 2006).

The hydrodynamic actions are due to the sea currents and the waves. The sea currents caused by the tidal wave propagation in shallow water can be characterized by a horizontal velocity field, whose intensity decreases slowly with the depth. Adopting a Cartesian coordinate system (*x'*, *y'*, *z'*) with origin at the still water level and the z'-axis oriented downward (Fig. 2), the variation in current velocity with the depth is given by (DNV 2010)

$$V_{cue}(z') = V_{tide}(z') + V_{wind}(z')$$

$$V_{tide}(z') = V_{tide0}\cdot\left(\frac{h-z'}{h}\right)^{1/7}$$

$$V_{wind}(z') = V_{wind0}\cdot\left(\frac{h_0-z'}{h_0}\right) \tag{4}$$

where: *Vtide*(z') and *Vwind(z')* are the velocities generated by the tide and the wind; z' is the depth under the mean still water level; V_{tide0} and V_{wind0} are the tidal current and the wind-generated current at still water level; *h* is the water depth from the still water level (taken as positive); h_0 is a reference depth (e.g. equal to 20 m). In absence of site-specific measurements, the wind-generated current velocity may be taken equal to (DNV 2010)

$$V_{wind0} = 0.01\cdot V_{1hour}(z=10\text{ m}) \tag{5}$$

where V_{1hour} is the 1-hour mean wind velocity.

Waves act on the submerged structural elements and on the transition zone above the still water level; therefore the wave actions are due to the motion of the fluid particles and to the breaking waves, which may occur in shallow water conditions. In general, the wave height is a time-dependent stochastic variable, described by

• the significant wave height H_S, defined as four times the standard deviation of the sea elevation process. It is the measure of intensity of the wave climate as well as of the variability of the wave heights;

• the spectral peak period T_P, related to the mean zero-crossing period of the sea elevation process.

For the extreme event analysis, the significant wave height is defined as a function of the return period T_R (DNV 2010)

$$H_s = F_{H_s,max,1year}^{-1}\left(1-\frac{1}{T_R}\right) \tag{6}$$

where $F_{Hs,max,1year}$ represents the probability distribution function of the maximum annual significant wave height.

For the determination of the wave action, it is necessary to define an appropriate spectral density of the sea surface elevation. The characteristic spectral density of the specific sea-state $S(n)$ is defined by means of the parameters H_S and T_P and by an appropriate mathematical model. Usually the Jonswap spectrum is adopted for a developing sea, given by

$$S(n) = \frac{a\,g^2}{(2\pi)^2}n^{-5}\,exp\left[-\frac{5}{4}\left(\frac{n}{n_p}\right)^{-4}\right]\gamma^{exp\left[-0.5\cdot\left(\frac{n-n_P}{\sigma\cdot n_P}\right)^2\right]} \tag{7}$$

where: $n = 2\pi/T$ is the frequency (in Hz); $n_P = 2\pi/T_P$ is the peak frequency, a and g are constants; σ and γ are parameters dependent on H_S and T_P.

In general, the sea state is characterized by a distribution of the energy spectral density dependent on the direction of the wave components: this can be obtained by multiplying the one-dimensional spectrum $S(n)$ by a function that takes into account the directional spreading, and is symmetrical with respect to the principal direction of the wave propagation. In the numerical calculations, for the sake of simplicity, the wave kinematics are described by the linear wave theory applied to small-amplitude deep water waves, and the wave profile has been represented by a sine function.

The portion of the OWT exposed to wind action is composed by the support structure over the still water level and the turbine tower. Well-known relations are adopted to model the wind actions (Simiu and Scanlan 1996). Since the tower is formed by a tubular member, the vortex shedding effect has been considered as the impressed maximum across-wind displacement $(r^{VS}_{across})_{max}$ given in Borri and Pastò (2007).

$$\left(\frac{r^{VS_{across}}}{D}\right)_{max} = \frac{1.29}{[1+0.43\cdot(2\pi\cdot S_t^2\cdot S_c)]} \tag{8}$$

where D is the diameter of the tubular section under wind action and S_t and S_c are the Strouhal and Scruton numbers (Simiu and Scanlan 1996). r^{VS}_{across} has been imposed to the node located at the hub height, when the mean wind speed falls within the critical vortex shedding range, defined by the vortex shedding critical velocity $V^{VS}_{crit} \pm 0.5$ m/s.

With reference to the hydrodynamic actions, if a slender cylindrical member ($D/L < 0.2$, where D is the member diameter normal to the fluid flow and L the wave length) is considered, the waves and sea currents generate the following forces per unit length:

• a force acting in the direction normal to the axis of the member, generated by the orthogonal components of the water particle velocity (sum of the wave v_w and current V_{cur} velocities) and by the wave acceleration; the force can be estimated by means of Morison's equation

$$dF(z',t) = \left(c_i\frac{\rho_{wat}\pi D^2}{4}\dot{v}_w(z',t) + c_d\,\rho_{wat}\,D\cdot\frac{1}{2}(v_w(z',t)+V_{cur}(z',t))\left|v_w(z',t)+V_{cur}(z',t)\right|\right)dz' \tag{9}$$

where ρ_{wat} is the water density, c_i and c_d are the inertia (including added mass) and drag coefficients, which are related to the structural geometry, flow conditions and surface roughness (a dot indicates the time derivative). Periodic functions are adopted for describing both wave velocities and accelerations (Brebbia and Walker 1979);

• a non-stationary (lift) force acting in the direction normal to the axis of the member and to the water current. This force is induced by vortex shedding; however, this force has been disregarded in the numerical calculations.

The wind-wave-sea current interaction can be roughly modeled by considering that:

• the wind velocity generates an additional sea current given by Eq. (5);

• the wind and the sea current velocities are statistically correlated both in direction and intensity; in the numerical calculations it has been assumed that the directions of wind and sea currents are perfectly correlated;

• the wind speed and the wave characteristic height are statistically correlated. The correlation has been modeled by a deterministic relation based on the correlation data reported in (Zaaijer 2006). Although the wave height has been scaled in order to consider Mediterranean waves instead of ocean waves, the decreasing factor has been calibrated by the Italian Wave Atlas (APAT 2004). Therefore the relation between V_{10} and H_S is given by

$$H_S = \frac{1}{2}(0.221 \cdot V_{10}^2 - 0.0291 \cdot V_{10} + 0.164) \qquad (10)$$

3. Analyses on an offshore wind turbine

The risk assessment of an OWT with a jacket support is considered as a case study. The jacket is composed by tubular steel members: the diagonal bars have a diameter of 0.5 m and a thickness of 0.016 m; the vertical bars have a diameter of 1.3 m and a thickness of 0.026 m; the horizontal bars have a diameter of 0.6 m and a thickness of 0.016 m. The tower is a tubular steel member with a circular section having a diameter of 5 m and a thickness of 0.05 m. With reference to the diagram in Table 1, the hub height over the still water level H is equal to 100 m, the water depth h to 35 m and the rotor radius R to 45 m. The turbine is a 3MW Vestas type (its characteristics are described in detail at the web site: http://www.vestas.com). The connection between the jacket and the tower is rigid. Table 1 illustrates the main structural properties.

Table 1 Main structural properties of the OWT

H = 100 m (hub height above the still water level)
h = 35 m (mean water depth from still water level)
D = 5 m
t_w = 0.05 m
Jacket members:
D_{vert} = 1.3 m
$t_{w\,vert}$ = 0.026 m
D_{hor} = 0.6 m
$t_{w\,hor}$ = 0.016 m
D_{diag} = 0.5 m
$t_{w\,diag}$ = 0.016 m
D = tower diameter
$D_{vert,\,hor,\,diag}$ = diameter of the vertical, horizontal and diagonal members of the jacket
t_w = thickness of the tower tubular member
$t_{w\,vert,\,hor,\,diag}$ = thickness of the vertical, horizontal and diagonal members of the jacket

In the numerical analyses, only the configurations that do not imply the rotation of the blades have been considered (that is, the parked - standstill and idling configurations). The structural analyses are carried out in the frequency domain and the probabilistic characteristics of the response parameters are derived by Monte Carlo simulation. A 3D finite element model of the structure is implemented in ANSYS (www.ansys.com), where the tower is modeled with beam elements and the jacket members are been modeled with truss elements. The turbine hub and the blades are taken into account only as equivalent masses.

3.1 Characterization of the stochastic parameters

The characteristics of the random parameters are synthesized in Table 2. The three components of the Intensity Measure vector **IM** are:
• the 10-minute mean wind speed V_{10} evaluated on an annual basis at 10 m height and characterized by a Weibull distribution;
• the roughness parameter z_0, characterized by a Lognormal distribution;

Table 2 Stochastic properties of IM, IP and SP parameters

	Stochastic variable	Description	Distribution type and parameters
IM	V_{10} [m/s]	Mean wind velocity at 10 m height	Weibull $k = 2.02$ (shape parameter) $\sigma^* = 6.2$ (scale parameter)
	α [deg]	Direction of mean wind velocity	Gaussian $\mu = 0$, $\sigma = 30^\circ$
	z_0 [m]	Roughness length	Lognormal $\mu = 0.02$, $\sigma = 0.03$
IP	St	Strouhal number	Lognormal $\mu = 0.22$, $\sigma = 0.025$
	ξ [%]	Structural damping	Lognormal $\mu = 0.05$, CoV= 0.08
	E [MPa]	Elastic modulus of steel	Lognormal $\mu = 205900$, CoV= 0.04
	D [m]	Tower diameter	Lognormal $\mu = 5$, CoV= 0.04
SP	t_w [m]	Thickness of the tower cross section	Lognormal $\mu = 0.05$, CoV= 0.04
	A_{vert} [m^2]	Cross-section of vertical jacket trusses	Lognormal $\mu = 0.104$, CoV = 0.04
	A_{diag} [m^2]	Cross-section of diagonal jacket trusses	Lognormal $\mu = 0.0294$, CoV = 0.04
	A_{hor} [m^2]	Cross-section of horizontal jacket trusses	Lognormal $\mu = 0.0243$, CoV =0.04

• the direction of the mean wind velocity α, characterized by a Gaussian distribution.

Concerning the interaction parameters **IP**, only the Strouhal number St is characterized as a random variable with a Lognormal distribution, while, the components of the Structural Parameters **SP** (all characterized by Lognormal distributions) are:
• the diameter D of the tower;
• the thickness t_w of the tower cross section;
• the cross sections of the vertical A_{vert}, horizontal A_{hor} and diagonal A_{diag} members of the jacket;
• the modulus of elasticity E of the steel;
• the structural damping ξ.

With regard to the structural response, three Engineering Demand Parameters *EDPs* are considered, all evaluated at the hub height:
• the mean value of the along-wind displacement;
• the peak value of the along-wind displacement;
• the peak value of the across-wind displacement.

The peak value of a response parameter r is evaluated as:

$$r^p = r_m + g_r \cdot \sigma_r \qquad (11)$$

where r_m is the mean value of r (corresponding to the mean wind velocity), σ_r is the standard deviation (evaluated by the power spectral density of the considered EDP), and g_r is the peak factor. The response is described by a Gaussian distribution; therefore, following Davenport (1998), the peak factor is equal to

$$g_r = \sqrt{2 ln(\eta \cdot T_{wind})} + \frac{0.577}{\sqrt{2 ln(\eta \cdot T_{wind})}} \qquad (12)$$

where: η is the cycling rate of the effective frequency of the response, equal to the first natural frequency n_1 of the structure; T_{wind} is the time interval over which the maximum value is evaluated. In the numerical analyses illustrated in the following, $n_1 = 0.428$ Hz; $T_{wind} = 3600$ s; therefore, $g_r = 3.9825$.

3.2 Analyses output

The output of the analyses are in the form of:
• the parameters of the distribution of the EDPs;
• the mean frequency λ(EDP) of exceeding the values of any EDP, that are assumed to give approximate values of the complementary cumulative distribution function G(EDP) defined in Eq. (1).

4. Analysis results

Sensitivity analyses have been carried out to investigate the influence on the risk assessment of the uncertainty of the input parameters (**IM** and **IP**) and the structural characteristics (**SP**).

A first series of sensitivity analyses (Table 3: sets 1-4) considers only the significance of the input

parameters **IM** and **IP**.

In each set of analyses, only one element of **IM** or **IP** is assumed as random, while the other parameters are deterministic. Each Monte Carlo simulation implies 500 samples. To evaluate the relevance of the uncertainty characterizing the wind actions, the hydrodynamic action is modeled as an equivalent static force, whose intensity depends on the mean wind velocity as described in Ciampoli and Petrini (2010).

In Figs. 3-7 the results of the sets of analyses 1-3-4 (Table 3) are shown; the set 2 gives results with the same trend of set 1. In Figs. 3-4, the variation of the across-wind displacements due to vortex shedding can be appreciated, for wind velocity falling in the critical vortex shedding range; the values of the along-wind and across-wind displacements increase with V_{10}. Similar results are obtained for the analysis sets No. 3 and 4.

Fig. 5 shows that the random variation of direction has no influence on the peak values of the along-wind and across-wind displacements due to the symmetry of the structure. When the Strouhal number S_t is considered as a random variable (Figs. 6 and 7), the critical vortex shedding range is not a deterministic interval, as in Fig. 3. As expected, the preliminary sensitivity analyses indicate that: V_{10} is the most relevant parameter; the uncertainty affecting the direction of the mean wind

Table 3 Preliminary sensitivity analyses−sets No. 1-5: IM and IP parameters considered, type of probability distribution and deterministic value (SP parameters deterministic)

| Analysis set	IM			IP
	V_{10}	z_0	α	S_t
1	Stochastic (Weibull)	Deterministic (= 0.02 m)	Deterministic (= 90°)	Deterministic (= 0.22)
2	Deterministic (= 19 m/s)	Stochastic (Lognormal)	Deterministic (= 90°)	Deterministic (= 0.22)
3	Deterministic (= 19 m/s)	Deterministic (= 0.02 m)	Stochastic (Gaussian)	Deterministic (= 0.22)
4	Stochastic (Weibull)	Deterministic (= 0.02 m)	Deterministic (= 90°)	Stochastic (Lognormal)
5	Stochastic (Weibull)	Stochastic (function of V_{10})	Stochastic (Gaussian)	Stochastic (Lognormal)
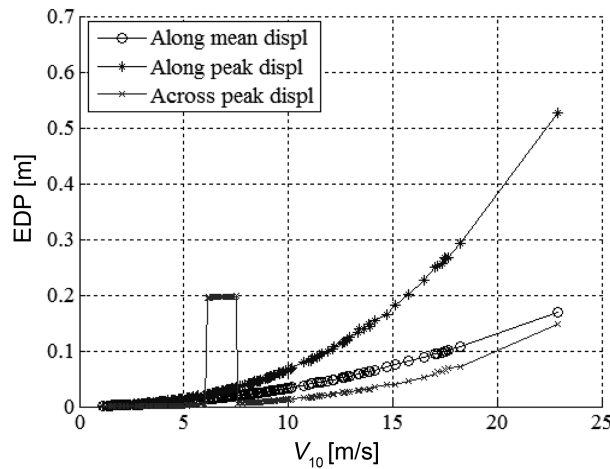
Fig. 3 Sensitivity analyses-set No. 1: assumed random variable: V_{10}: values of the EDPs
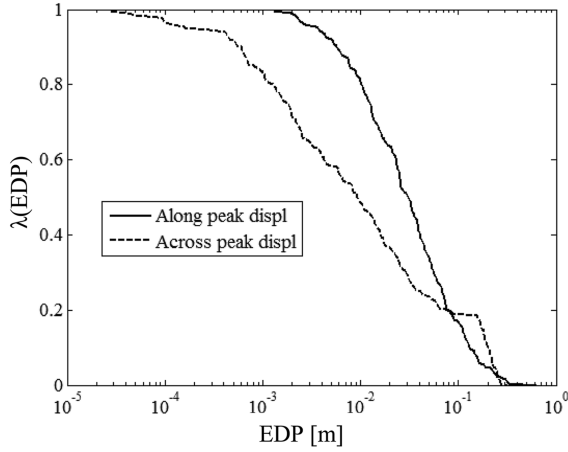
Fig. 4 Sensitivity analyses – set No. 1, assumed random variable V_{10}: mean annual frequencies $\lambda(EDP)$ of exceeding any value of the EDPs
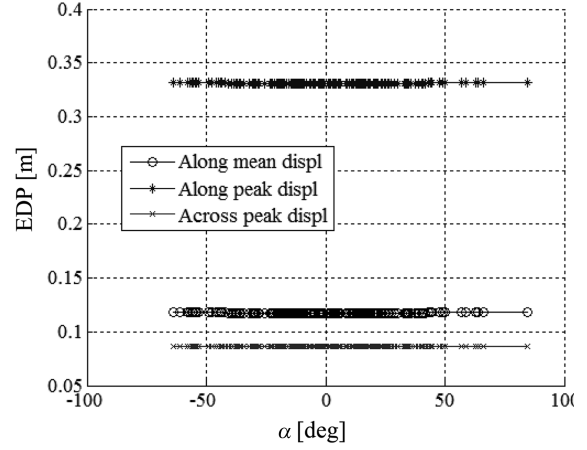

Fig. 5 Sensitivity analyses – set No. 3; assumed random variable: α; values of the considered EDPs
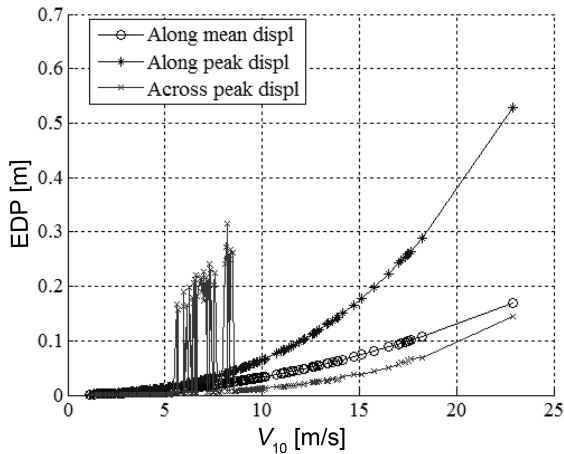

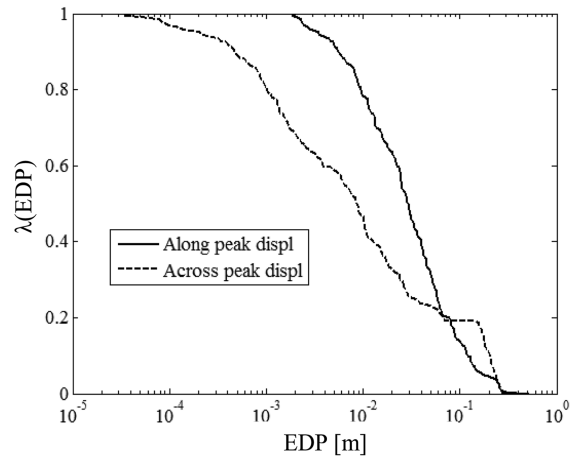Fig. 6 Sensitivity analyses – set No. 4: values of the considered EDPs

Fig. 7 Sensitivity analyses – set No. 4: mean annual frequencies $\lambda(EDP)$ of exceeding any value of the considered EDP

velocity is negligible for a symmetric structure; finally the uncertainty affecting the Strouhal number has a direct influence on the across-wind response. In the same figures also the risk curves defined by Eq. (1) are reported.

The set of analyses No. 5 assume that all **IM** and **IP** are random, while the **SP** parameters are considered deterministic. The results of the risk assessment are shown in Figs. 8 and 9.

Finally, in Figs. 10 and 11 a comparison between the mean annual frequencies $\lambda(EDP)$ obtained by the set of analyses 5 and the analyses carried out by considering the uncertainty of the **SP** parameters is reported. In order to improve the definition of the roughness length z_0, its value has been evaluated by the wave height H_S which depends on V_{10} by the relation
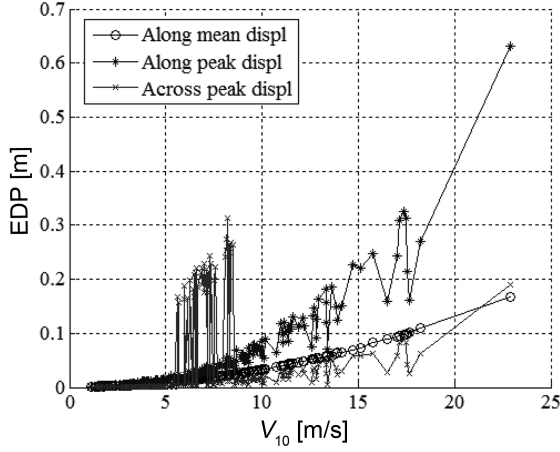
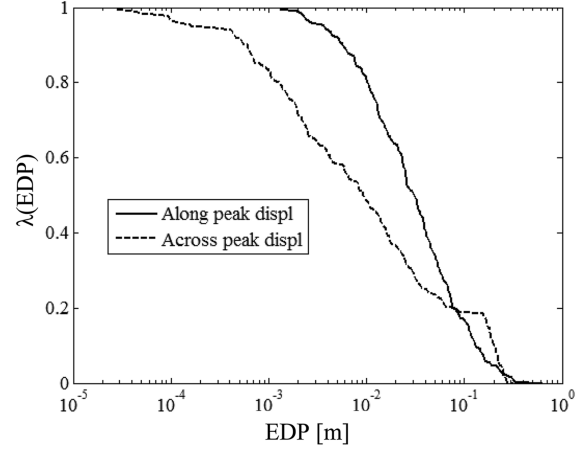Fig. 8 Sensitivity analyses −set No. 5: values of the considered EDPs as a function of V_{10}

Fig. 9 Sensitivity analyses −sset No. 5: mean annual frequencies λ(EDP) of exceeding any value of the considered EDP
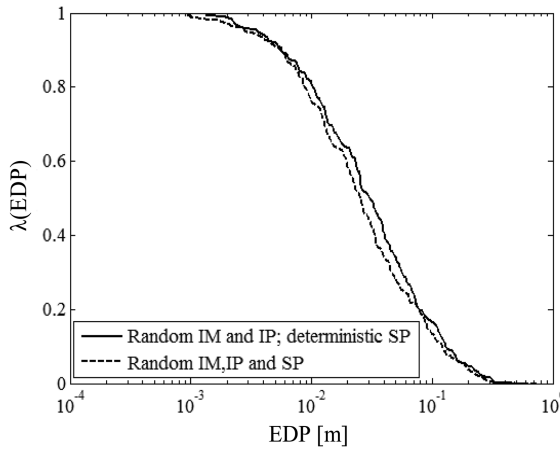

Fig. 10 Comparison of the mean annual frequencies λ(EDP) of exceeding any value of the peak along-wind displacement
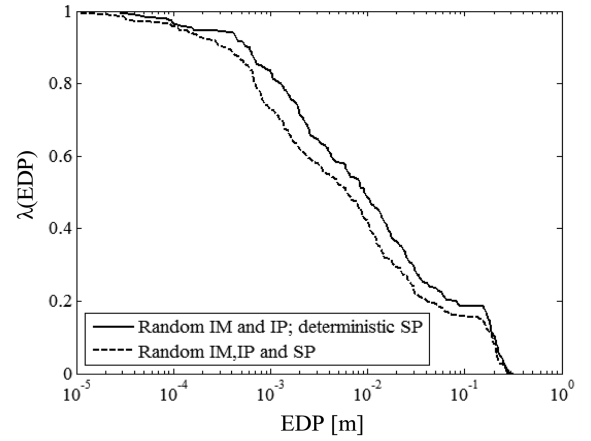

Fig. 11 Comparison of the mean annual frequencies λ(EDP) of exceeding any value of the peak across-wind displacement by disregarding or considering the uncertainty of the SP.

$$z_0 = 0.03 + \frac{0.04}{9.81}\left[V_{10} \cdot \frac{0.4}{\ln(10/z_0)}\right]^2 \tag{13}$$

which is a modified version of the equation proposed in Holmes (2001).

Finally, in Fig. 12 the maximum values of the normal forces in the vertical members of the jacket are reported: they correspond to an admissible state of stresses.

Looking at the two sets of plots, it appears evident that the risk assessment, if expressed in terms of the displacements in the along-wind direction, does not change significantly. On the contrary, if the risk is expressed in terms of the displacements in the across-wind direction, a reliable assessment requires that all relevant parameters (including **SP** parameters) are considered as random.
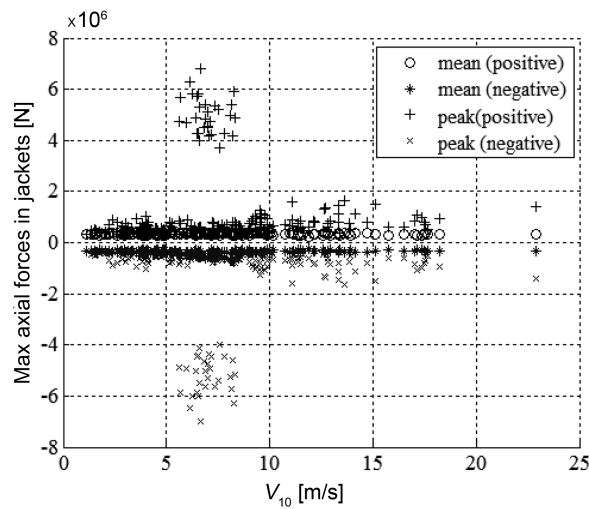
Fig. 12 Values of the maximum normal forces in the vertical trusses.

5. Modeling of the wind induced stress on the hub

In order to obtain a detailed description of the actions produced on the hub by each of the three rotating blades, a meso-level model of the single blade is developed. As stated before, with respect to macro-level models, meso-level models take into account the effects obtained by a more detailed description of the shape of the structural components. The required level of shape detail can be obtained using planar (shell) structural finite elements (Fig. 13). In this study, the blade considered has a length of 37 meters and the wind is modeled acting at eight locations along the blade. The main goal is to compute some main reaction forces between the single blade and the hub, in particular the reactions Ry contrasting the wind drag forces and the moment Mz contrasting the overturning moment acting on the blade (Fig. 14). The FE model of the blade is also shown,
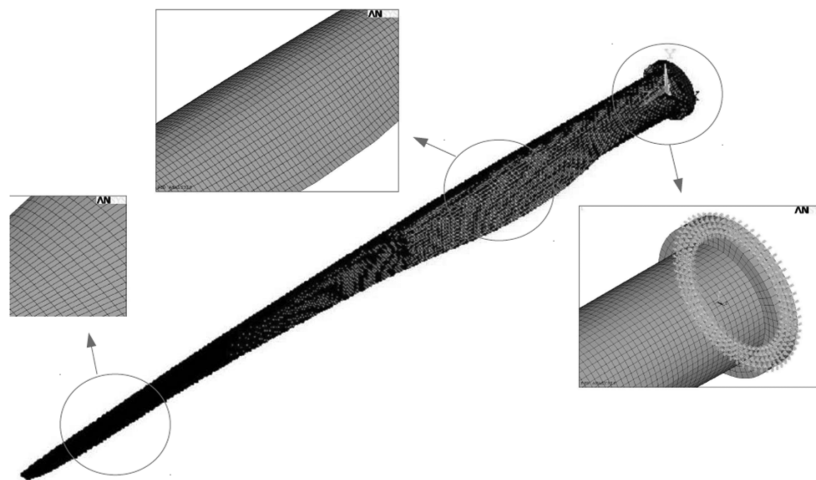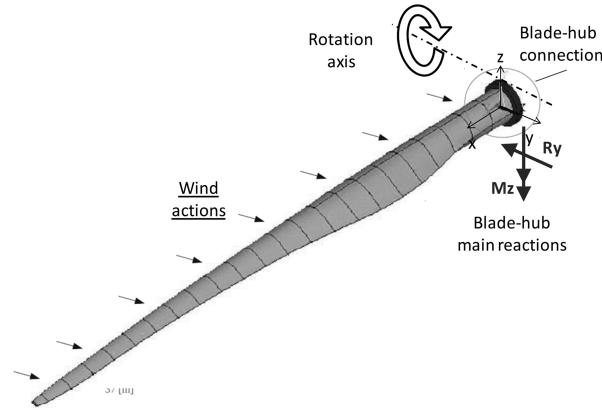

Fig. 13 FE model of the blade

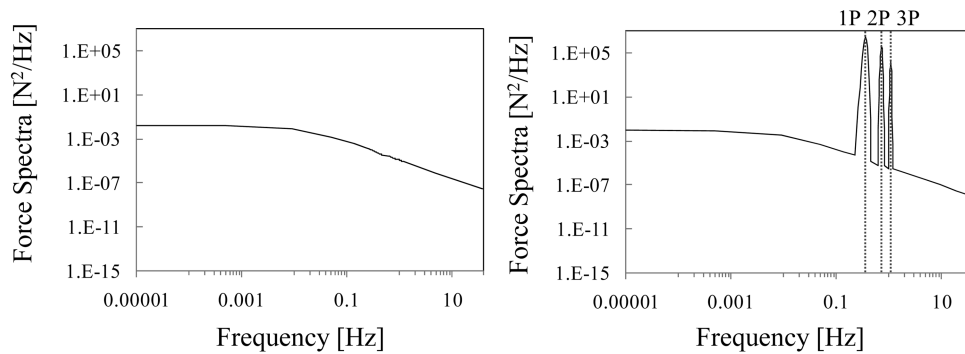Fig. 14 Main features of the meso-scale problem

Fig. 15 Acting wind force spectra: turbulent wind forces for parked turbine (left) and for rotating blades (right)

consisting in a 23750 shell finite elements. The wind turbulent action engaging the whole blade is modeled implementing an eight-variate Gaussian stochastic process.

The effects of the blade rotational motion has been taken into account by superposing a so called "rotating force spectrum" to the wind turbulence action spectrum. The rotating force spectrum is the one described in Murtagh et al. (2005) and Dueñas-Osorio and Basu (2008) as re-elaborated in De Gaudenzi (2011). The rotating force spectrum corresponding to the transit of the same blade (or one of the three rotating blades) in a certain location has been modeled by considering a single harmonic wind force having the fluctuating period equal to the time interval occurring between the first and second blade transit in that specific location during its rotational motion. The analyses have been carried out in the frequency domain and the turbulent wind spectra has been computed as described earlier by considering a V_{10} equal to 10 m/s.

An example of wind force spectra acting in one of the 8 considered locations along the blade is shown in Fig. 15 where the wind force spectra acting in the case of a parked turbine is also shown. 1P, 2P, 3P are the frequencies corresponding to the transit of the blades in the same location in case of rotor with one- two or three blades. The values obtained for the standard deviations of Fy and Mz are 20110 N and 51900 Nm respectively. These results can be useful for more detailed calculations, e.g., for fatigue life assessment of wind turbine components.

6. Conclusions

This paper focuses on the effects on the structural response of an OWT of the uncertainty in the parameters used to describe the environmental actions and the finite element model of the structure (herein referred to as modeling parameters). A proper probability characterization of the parameters is assumed, and the relevance and the propagation of the uncertainty to the response are investigated. Reference is made to an OWT with a jacket support structure.

The relevance of the various uncertain parameters is assessed by evaluating the structural risk, expressed by the probabilities of exceeding threshold values of the peak across-wind and along-wind displacements at the hub height. As expected, the mean wind velocity V_{10} is the most relevant environmental parameter; the uncertainty affecting the direction of the mean wind velocity is negligible for a symmetric structure and the uncertainty affecting the Strouhal number has a direct influence on the across-wind response. Moreover, if the risk is expressed in terms of the peak displacements in the across-wind direction, a reliable assessment requires that all relevant parameters (including the structural parameters) are considered as random. A procedure for the accurate modeling of the wind-induced stress on the hub is also provided. Some observations can be made about this procedure, which is an integral part of the multi-level approach. In a first place, blade FE modeling can be very complex due to the complex geometry. Furthermore, different models are available, with a vast diversity in the geometry and size. In this sense, the blade implemented in this study can be considered merely as a case study.

Acknowledgements

References

APAT - Agenzia per la Protezione dell'Ambiente e per i Servizi Tecnici (2004), "Atlante delle onde nei mari italiani – Italian Wave Atlas", Rome, Italy (in Italian).

Arangio, S. and Beck, J.L. (2010), "Bayesian neural networks for bridge integrity assessment", *Struct. Health Monit.*, **19**(1), 3-21.

Arangio, S. and Bontempi, F. (2010), "Soft computing based multilevel strategy for bridge integrity monitoring", *Comput - Aided Civil. Inf.*, **25**(5), 348-362.

Arangio, S., Bontempi, F. and Ciampoli, M. (2011), "Structural integrity monitoring for dependability", *Struct. Infrastruct. E.*, **7**(1-2), 75-86.

Bontempi, F. (2006), "Basis of design and expected performances for the Messina Strait Bridge", *Proceedings of the International Conference on Bridge Engineering – Challenges in the 21st Century*, Hong Kong, 1-3 November.

Borri, C. and Pastò, S. (2006), *Lezioni di ingegneria del vento*, Firenze University Press, Firenze (in Italian).

Brebbia, C.A. and Walker, S. (1979), *Dynamic analysis of offshore structures*, Nwenes-Butterworths, London.

Breton, S.P. and Moe, G. (2009), "Status, plans and technologies for offshore wind turbines in Europe and North

America", *Renew. Energ*., **34**(3), 646-654.

Carassale, L. and Solari, G. (2006), "Monte Carlo simulation of wind velocity field on complex structures", *J. Wind Eng. Ind. Aerod*., **94**(1), 323-339.

Ciampoli, M. and Petrini, F. (2010), "Performance-based design of offshore wind turbines", *Proceedings of the 12th International Conference on Engineering, Science, Construction, and Operations in Challenging Environments*, (Eds. Song, G. and Malla, R.B.), Honolulu, HI, March 14–17.

Ciampoli, M., Petrini F. and Augusti, G. (2011), "Performance-based wind engineering: towards a general procedure", *Struct. Saf*., **33**(6), 367-378.

Davenport A.G. (1998), "Probabilistic methods in wind engineering for long span bridges", *Proceedings of the International Symposium on Advances in Bridge Aerodynamics*, Copenhagen, Denmark.

De Gaudenzi, O. (2011*), Energy harvesting in civil structures under wind action: application of piezoelectric devices*, Laurea Magistrale Thesis, Department of Structural and Geotechnical Engineering, Sapienza Università di Roma, Rome, Italy.

DNV - Det Norske Veritas (2010), DNV-OS-J101 Offshore Standard. Design of Offshore Wind Turbine Structures.

Dueñas Osorio, L. and Basu, B. (2008), "Unavailability of wind turbines due to wind-induced accelerations", *Eng. Struct*., **30**(4), 885-893.

Giuliani, L. and Bontempi, F. (2010), "Structural integrity evaluation of offshore wind turbines", *Proceedings of the 12th International Conference on Engineering, Science, Construction, and Operations in Challenging Environments*, (Eds. Song, G. and Malla, R.B.) Honolulu, HI, March 14–17.

Hau, E. (2006), *Wind turbines: fundamentals, technologies, application, economics*, 2nd, Ed., Springer-Verlag Berlin Heidelberg.

Holmes, J.D. (2001), *Wind loading of structures*, Spoon Press, London.

Murtagh, P.J., Basu, B. and Broderick, B.M. (2005), "Along-wind response of a wind turbine tower with blade coupling subjected to rotationally sampled wind loading", *Eng. Struct*., **27**(8), 1209-1219.

Petrini, F. (2009), *A probabilistic approach to performance-based wind engineering*, Ph.D. dissertation,

Department of Structural and Geotechnical Engineering, Sapienza Università di Roma, Rome, Italy.

Petrini, F. and Ciampoli M. (2011), "Performance-based wind design of tall buildings", *Struct. Infrastruct. E*.

Petrini, F., Li, H. and Bontempi, F. (2010a), "Basis of design and numerical modeling of offshore wind turbines", *Struct. Eng. Mech*., **36**(5), 599-624.

Petrini, F., Manenti, S., Gkoumas, K. and Bontempi, F. (2010b), "Structural design and analysis of offshore wind turbines from a system point of view", *J. Wind Eng. Ind. Aerod*., **34**(1), 85-108.

Simiu, E. and Scanlan, R.H. (1996), *Wind effects on structures,* 3rd Ed., John Wiley & Sons, New York.

Zaaijer, M.B. (2006), "Foundation modeling to assess dynamic behaviour of offshore wind turbines", *Appl. Ocean Res*., **28**(1), 45-57.